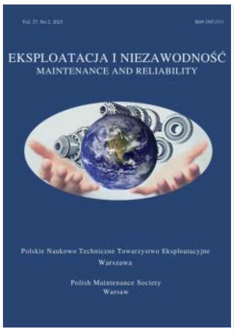

Eksploatacja i Niezawodnosc – Maintenance and Reliability

Volume 27 (2025), Issue 2

journal homepage: http://www.ein.org.pl

Article citation info:
Liu Y, Enhancing Flexibility and Reliability in Smart Distribution Networks: A Self-Healing Approach, Eksploatacja i Niezawodnosc – Maintenance and Reliability 2025: 27(2) http://doi.org/10.17531/ein/195269

Indexed by: Web of Science Group

Enhancing Flexibility and Reliability in Smart Distribution Networks: A Self-Healing Approach

Yuan Liu[a,*]

[a] State Grid Henan Information & Telecommunication Company，State Grid Henan Electric Power Company，Zhengzhou 450000，China

Highlights

- Modeling of self-healing in a smart distribution network with integrated microgrids.
- Restoration patterns and planning profiles patterns considering errors in microgrids.
- Autonomous distributed restoration technology through a multi-agent system.
- Reliable solver with low solution deviation,enhancing security in reconstruction process.
- Flexibility in the smart distribution network for effective operation and management.

Abstract

This paper presents a pioneering approach that integrates a Self-Healing System through a Smart Distribution Network, which employs a two-step implementation of a comprehensive Energy Management algorithm and a multi-agent system with an autonomous distributed regeneration method. The novel method improves network operation through optimized management of local microgrids, which include diverse components comprising renewable energy sources, electric vehicle charging infrastructure, and energy storage systems. The first phase concentrates on minimizing network operation costs by adhering to system utilization restrictions and optimal load distribution, while the second phase addresses the optimization of regeneration processes, which decreases discrepancies between recoverable priority loads and switching operations. The evaluation introduces a stochastic programming approach to model and manage uncertainties, and utilizes the Kantorovich method and the roulette wheel mechanism to improve reliability. The proposed student psychology-based optimization algorithm ensures reliable solutions to complex non-linear problems. Numerical outputs highlight the effectiveness of the recovery strategy, which depicts successful management of line current and voltage through allowable limits, and a reduction in expected unsupplied energy from 108.48 kWh to 7.21 kWh. This approach not only advances the smart grid framework but also remarkably improves the reliability of neighborhood microgrids.

Keywords

autonomous distributed regeneration, energy management algorithm, multi-agent systems, Self-Healing system, smart distribution network.

1. Introduction

1.1. Background and Aims

In an isolated microgrid, meeting load demand is challenging because of the variable output of renewable energy sources (RES) comprising wind and solar systems. This uncertainty, combined with load variability, can bring out overloading problems in microgrids [1]. To overcome this issue, various strategies have been introduced, comprising integrating energy storage units, and non-renewable energy sources including diesel generators and microturbines, which are connected to the main grid, and the interconnection of the neighboring

(*) Corresponding author.
E-mail addresses: Y. Liu (ORCID: 0009-0008-2475-5834) haoshihuasheng924@126.com

microgrids [2]. It would probably raise the operation cost in an off-grid microgrid due to the energy storage systems or the usage of other non-renewable energy sources, because of maintenance and fueling concerns [3]. On the other hand, in a grid-connected microgrid, despite having very high uncertainties, the system flexibility is low due to the high operational costs. However, the coordination of neighboring microgrids has been proved as a reliable and economical solution for overload management in microgrids [4]. Such hybridization includes a new strategy of static switches interconnecting each pair of adjacent microgrids. In cases of overload, such switches are on to shift some powers from one microgrid to another. As this method tends to relieve the overload problem, it also improves the overall system reliability by preparing the backup power for further improvement in response times to demand oscillation [5]. This will be an inclusive solution to ensure that the energy network will be resilient enough to take on the changed load and generation patterns. Advanced control algorithms, together with communication methodologies, are implemented in optimization of the operation of the interconnected microgrid through assurance of high efficiency in power distribution and the reduction of the possibility of cascading failures [6]. These will allow for real-time monitoring and dynamic adjustment of power flows, extending the capability of the system to react to changes in situation and stability. Applied through hybridization with neighbor microgrids, it will mean a flexible energy framework with the cancelation of current and future problems characterizing power management.

1.2. Literature review

There are various works related to the search for other forms of self-healing approaches with views to enhance smart distribution networks in terms of reliability and flexibility. In these papers, different methods have been followed to make the distribution units resilient and adaptive. The following is the literature survey that collects some key contributions of this research field and focuses on different methodologies and their impacts on network performance.

Wong et al. [7] presented the incorporation of self-healing into smart distribution networks through adaptive protection schemes. They established that such a scheme can achieve a dynamic reduction in fault down time and improve reliability. They presented a methodology that utilized real-time data to perform settings protection and isolation of faults in an effective way. Yavuz et al. [8] conducted research on a novel self-healing algorithm based on machine-learning approaches for smart grids. The authors focused on predictive fault-detection methods to increase the flexibility of the system. The proposed algorithm was able to use previous history in making necessary predictions for possible failures and utilizing proactive measures. Srivastava et al. [9] studied the decentralized self-healing mechanism and implemented multi-agent units. Their method enabled the possibility of distributed decision-making for fault detection and increased flexibility and reliability. Each agent in the system acted independently to handle local problems while coordinating with others. Arefifar et al. [10] studied the application of strategies of real-time monitoring and control, improving self-healing capabilities in distribution networks. They pointed out the use of modern sensors and communication techniques in fault diagnosis and response quickly. These methods put together enable isolation of faults and restoration of service in a very short time. Esmaeil et al. [11] discussed the role of smart switches to build self-healing distribution networks. They mentioned that the smart switch can reconfigure the network by itself in order to bypass the fault to continue the service. They underlined the importance of real-time communication between the switches in case of a fault. Wong et al. [12] researched the applications of adaptive protection schemes to enhance the self-healing capability of smart distribution networks. Emphasis is placed on the dynamic updating of protection settings with a view to real-time network conditions. Under their proposal, the isolation of faults was improved, thereby reducing service interruptions. This flexibility is very important to ensure a reliable power supply during disturbances in the network.

Aldrini et al. [13] discussed a self-heating scheme and adopted a combination of automated fault detection with remote-control systems. They gave the advantages of coupling these units in order to enhance the resilience of the network. Their study demonstrated that coupled automated fault detection with remote control has the possibility to restore the service in a shorter time. Mahmoud et al. [14] addressed the use of artificial intelligence in selfhealing distribution networks.

They used AI algorithms for fault detection in real time and concluded that AI can enhance a network's capability for autonomous response against faults. Kuo [15] analyzed the integration of energy storage systems into self-healing distribution networks. Their results showed that energy storage might provide a contribution to fault recovery and stabilize the grid during disturbances. They have also discussed the contribution of the storage systems in the improvement of the network reliability. Zakaryaseraji et al. [16] discussed the introduction of electric vehicles and renewable energy sources, hence addressing challenges for power system optimizations. Their reports were presenting ways of optimizing the EV charging methods and distributed generation (DG) placement considering the probabilistic effects of renewable sources. Their technique lessened the congestion on the network and improved ATC, while cost-based techniques convinced customers to reshape their consumption, thereby improving overall grid stability. Shittu et al. [17] presented a self-healing framework that is dependent upon integrating distributed generation sources. They demonstrated that distributed generation can improve network resilience by providing backup power during faults. Their research underlined that coordination at large distribution of resources is necessary in self-healing.

Nahi et al. [18] assessed the possibility of using demand response techniques to give the network self-healing capabilities. In this regard, they mentioned that once faults happen, balancing the network after demand variations avoids overloads. Their findings showed that demand response techniques improve the reliability at the network level. Sardashti and Ramezani [19] discussed fault tolerant control systems applications on smart grids. They emphasized that such systems can keep the operation of the network even though these faults are experienced. The research study has shown the contribution of the fault-tolerant control towards increasing the dependability of the system. El-Tawab et al. [20] researched the impact of grid reconfiguration in self-healing distribution networks. They contended that network reconfiguring can isolate fault points and thereby restore service in a far more effective manner. Their work identified the benefits that dynamic network reconfiguration has when used in order to enhance flexibility and reliability. Shyama et al. [21] investigated a self-healing strategy that integrated network topology optimization with fault detection methodologies. They reported that it is possible to enhance network topology optimization in order to improve fault management and recovery and presented the impact of the hybridized approach on improving the network's flexibility and reliability. Aldrini et al. [22] investigated the use of real-time analytics for enhancing self-healing capabilities in smart distribution networks. They mentioned that real-time data assessment allows for prompt fault identification and intervention across the networks. From the results, it was observed that real-time analytics increases flexibility in the network due to timely intervention that enhances reliability. Guan et al. [23] focused on deploying automated restoration strategies in self-healing distribution networks and discussed that the automated units would restore power after faults in very little time. Their reports unmasked that automation would minimize the loss due to reduced downtimes, hence improving network reliability. Fan et al. [24] based on the study aimed to discuss the impact of communication protocols, inspected some of the functionality of self-healing capability in smart grids. They informed that effective communication schemes can make the detection and response against faults, and also robustness in communications is one of the key approaches for the improvement in network flexibility and reliability. Thirunavukkarasu et al. [25] proposed a hybrid optimization techniques-based selfhealing scheme. They have demonstrated that the hybrid optimization technique of various optimization techniques can improve the fault management and recovery. The research concluded that hybrid optimization improves the network flexibility. Hasankhani et al. [26] also addressed the issue of utilizing blockchain to improve self-healing techniques in a smart distribution network. They concluded that blockchain would enable secure and transparent fault management, and they focused on the potentiality of blockchain to increase the reliability of the network.

1.3. Literature Gap and Research Contribution

Despite remarkable advancements in self-healing systems for smart distribution networks (SDNs), plenty of existing research gaps still remain unsolved. Numerous studies concentrate on individual methods comprising adaptive protection schemes, multi-agent systems, and fault detection algorithms, but there is a lack of comprehensive integration through a unified framework. Most of the approaches that exist basically address only fault isolation and recovery, with hardly any consideration given to the optimization of coordination between the local microgrids and the wider distribution network during continued functioning. There is also a general lag in investigating how RESs, EVs, and ESSs will interactively affect the flexibility and reliability of the network under fault conditions. Besides, the uncertainties related to renewable generation and oscillation of loads are normally ignored, and subsequently demanding the robustness of stochastic modeling in light of such complexities. Moreover, most existing reconstruction strategies fail to consider neighboring microgrids and key distribution system constraints like voltage and current limits, which are crucial for effective power load distribution during recovery. This paper addresses these gaps by introducing a novel two-stage EM algorithm and an SHS through an SDN that hybridizes neighboring microgrids employing autonomous distributed restoration technology. The first stage optimizes operational costs by managing load distribution across RES, EVs, and ESSs while complying with system constraints. The second stage focuses on lessening the differences between switching operations and recovered priority loads under fault conditions. Furthermore, this research utilizes a multi-agent system to coordinate between overloaded and non-overloaded microgrids, which elevates overall flexibility and reliability. To manage uncertainties, a stochastic programming approach is applied, while utilizing the Kantorovich method and roulette wheel mechanism to guarantee reliable restoration. This comprehensive framework improves resilience and optimizes the recovery process in interconnected microgrid environments. Besides, the key contributions of this research can be listed as follows:

1. The presented study brings out an innovative fusion of SHS with SDN, which improves the network's ability to self-regenerate and manage faults effectively.
2. The study advances the field by implementing a two-step EM algorithm designed for optimized network operation and efficient neighborhood microgrid management.
3. Introduction of a multi-agent system with autonomous regeneration capabilities, to minimize recovery discrepancies and optimize switching operations.
4. Utilization of stochastic programming methods, such as the Kantorovich method and roulette wheel mechanism, to model and manage uncertainties, to elevate the reliability of the network.
5. Application of a novel optimization algorithm inspired by student psychology to overcome complex non-linear problems, which ensures effective and reliable solutions.

2. Problem statement

2.1. The first stage of optimization

In the realm of electrical distribution systems, optimization of microgrid reconstruction and planning is a vital goal. This pursuit is reinforced by the overall goal of minimizing the projected energy costs associated with the distribution system. As stated in Eq. (1), in the first step, the objective function is carefully formulated to reduce the expected energy cost in the distribution system. This effort directly targets the upstream grid and is according to the assumption that local power sources are equipped to meet the energy requirements of the smart distribution grid. This approach, in turn, emphasizes the redistribution of excess power generated by microgrids to decrease the electrical load on neighboring microgrids (CNMG) [5]:

$$\mathrm{Min}\ \sum_{\omega} \pi(\omega) \times \sum_{t}\left[\lambda(t,\omega) \times P_{Ref}^{S}(t,\omega)\right] \tag{1}$$

This optimization problem is supported by a series of fundamental constraints that guarantee the integrity and efficiency of the electrical distribution system.

The creation of AC load distribution equations, such as Eqs. (2) to (7), and figuring out the intelligent distribution network's working constraints, including Eqs. (8) to (10), are among the outlined limitations in this part. Important components of AC load distribution equations include size and angle parameters, active and reactive power load distribution (Eq. (4) and Eq. (5)), and nodal active and reactive power balance (Eq. (2) and Eq. (3)). The voltage at the slack bus is included (Eq. (6) and Eq. (7)). Simultaneously, the distribution bus capacity (Eq. (8)), distribution line capacity (Eq. (9)), and voltage constraints (Eq. (10)) are only a few of the many factors that make up the SDN's operational limitations [5]:

$$P_D(n,t,\omega) = P_S(n,t,\omega) + \sum_m P_{MG}(m,t,\omega) \times B(n,m) - \sum_j P_L(n,j,t,\omega) \times A(n,j) \tag{2}$$

$$Q_D(n,t,\omega) = Q_S(n,t,\omega) - \sum_j Q_L(n,j,t,\omega) \times A(n,j) \tag{3}$$

$$P_L(n,j,t,\omega) = g(n,j) \times \left(V(n,t,\omega)\right)^2 - V(j,t,\omega) \times V(n,t,\omega) \times \{b(n,j) \times \sin\left(\delta(n,t,\omega) - \delta(j,t,\omega)\right) + g(n,j) \times \cos\left(\delta(n,t,\omega) - \delta(j,t,\omega)\right)\} \tag{4}$$

$$Q_L(n,j,t,\omega) = -b(n,j) \times \left(V(n,t,\omega)\right)^2 + V(j,t,\omega) \times V(n,t,\omega) \times \{-g(n,j) \times \sin\left(\delta(n,t,\omega) - \delta(j,t,\omega)\right) + b(n,j) \times \cos\left(\delta(n,t,\omega) - \delta(j,t,\omega)\right)\} \tag{5}$$

$$V(n,t,\omega) = V_{Ref} \qquad \forall n = \mathrm{Ref}, t, \omega \tag{6}$$

$$\delta(n,t,\omega) = 0 \qquad \forall n = \mathrm{Ref}, t, \omega \tag{7}$$

$$\sqrt{\left(P_L(n,j,t,\omega)\right)^2 + \left(Q_L(n,j,t,\omega)\right)^2} \le S_L^{Max}(n,j) \tag{8}$$

$$\sqrt{\left(P_S(n,t,\omega)\right)^2 + \left(Q_S(n,t,\omega)\right)^2} \le S_S^{Max}(n) \tag{9}$$

$$V^{Min} \le V(n,t,\omega) \le V^{Max} \tag{10}$$

The constraints for EVs are extended from Eqs (11) to (15) and represent various aspects such as the energy stored in EV batteries, energy levels at entry and exit, and active power constraints for charging and discharging [5]:

$$E_{EV}(m,t+1,\omega) = \eta_{Ch} \times P_{Ch}^{EV}(m,t,\omega) + E_{EV}(m,t,\omega) - P_{Dch}^{EV}(m,t,\omega) \times \frac{1}{\eta_{Dch}} \tag{11}$$

$$E_{EV}(m,t,\omega) = E^{Arr}(m,t,\omega) \qquad \forall m, t = \text{Arrival time}, \omega \tag{12}$$

$$E_{EV}(m,t,\omega) = E^{Dep}(m,t,\omega) \qquad \forall m, t = \text{Departure time}, \omega \tag{13}$$

$$0 \le P_{Ch}^{EV}(m,t,\omega) \le CR^{EV}(m) \times ev(m,t,\omega) \tag{14}$$

$$0 \le P_{Dch}^{EV}(m,t,\omega) \le DR^{EV}(m) \times (1 - ev(m,t,\omega)) \tag{15}$$

Similarly, the restrictions governing the operation of energy storage are set in a sequence that is expanded in Eqs (16) to (20). These equations include calculations of energy stored in energy storage batteries, initial stored energy, energy limits, and active power limits for charging and discharging operations [5]:

$$E_{ES}(m,t+1,\omega) = \eta_{Ch} \times P_{Ch}^{ES}(m,t,\omega) + E_{ES}(m,t,\omega) - P_{Dch}^{ES}(m,t,\omega) \times \frac{1}{\eta_{Dch}} \tag{16}$$

$$E_{ES}(m,t,\omega) = E^{Max}(m) \quad \forall m, t = 1, \omega \tag{17}$$

$$E^{Min}(m) \le E_{ES}(m,t,\omega) \le E^{Max}(m) \tag{18}$$

$$0 \le P_{Ch}^{ES}(m,t,\omega) \le CR^{ES}(m) \times es(m,t,\omega) \tag{19}$$

$$0 \le P_{Dch}^{ES}(m,t,\omega) \le DR^{ES}(m) \times (1 - es(m,t,\omega)) \tag{20}$$

A set of constraints expands its understanding to include neighboring microgrids and includes a comprehensive set of equations that underlie the operation of these fundamental components. As stated in Eq. (21), for each microgrid in neighboring microgrids, active power balance appears as a key factor. This equation highlights the balance between active loads and microgrid energy sources, which include EVs and ESSs.

$$P_{MG}(m,t,\omega) = \left(P_{Dch}^{ES}(m,t,\omega) - P_{Ch}^{ES}(m,t,\omega)\right) + \left(P_{Dch}^{EV}(m,t,\omega) - P_{Ch}^{EV}(m,t,\omega)\right) + P_{PV}(m,t,\omega) + P_W(m,t,\omega) - D_{MG}(m,t,\omega) \tag{21}$$

2.2. Second stage optimization

The optimization framework for the self-healing method is covered in this part. Its purpose is to determine and apply the best restoration pattern and scheduling profile in the event of a fault or microgrid overload. This step is preceded by the problem context from the previous stage. In this optimization issue, the goal function is to diminish the discrepancy between the quantity of switching operations and priority load recovery. This target, shown in Eq. (22), is normalized by coefficients w_1 and w_2 [5].

$$\mathrm{Min} \quad w_1 \sum_s |s\omega(s) - sw_0(i)| - w_2 \sum_\omega \pi(\omega) \times \sum_n W(n) \cdot x(n) \cdot P_D(n, t = \text{fault time}, \omega) \tag{22}$$

To enhance the recovery process, a set of constraints is applied, which depends on the integration of an automatic demand response technique based on a multi-agent energy system and overload management of neighboring microgrids in the fault. This strategy begins with the detection of an internal fault, which subsequently causes the feeder switch to shut down. This initiates the delineation of regions based on fault location and leads to their respective roles dictated by the multifactorial energy system. This technique includes four regional factors for the distribution network. The fault zone agent, designated as the decision agent, leads the reconstruction efforts, while the bottom zone agent, designed for areas lost due to faults, steps in. The healthy area in the repair path is provided by the healthy area agent, and the healthy area is placed under the authority of the area line agent with a switch. Further complexity appears in the form of regional agents specific to microgrids, which represent both types of overloaded microgrid regional agents and non-overloaded microgrid regional agents. As stated in Eq. (23), the radial structure of the distribution network acts as a basic principle and shows the relations between the number of feeder lines and feeder buses. As indicated in Eq. (24), the current limits imposed on all feeder lines are very important [5]:

$$\mathrm{N_{Bus}} = \mathrm{N_{Line}} + 1 \tag{23}$$

$$-\mathrm{I^{Max}}(\mathrm{j}) \leq \mathrm{I}(\mathrm{j}) \leq \mathrm{I^{Max}}(\mathrm{j}) \tag{24}$$

Voltage limits, both in healthy supply buses and in feeder buses, are prioritized to ensure the stability of the network, which is detailed in Eqs (25) and (26). In these equations, the magnitude of the impedance plays a key role [5]:

$$\mathrm{I_{VH}} = \frac{\mathrm{V_H} - \mathrm{V^{Min}}}{\mathrm{Z_H}} \tag{25}$$

$$\mathrm{I_{VF}} = \frac{\mathrm{V_T} - \mathrm{V^{Min}}}{\mathrm{Z_F}} \tag{26}$$

- **Error area factor**

The operation of the fault zone operator is based on certain conditions that indicate internal faults. The agent responds when the upstream or downstream input currents deviate significantly from their limits. In this scenario, the fault zone agent steps in to initiate the recovery process, isolating the fault using strategic switches through the zone. Simultaneously, the fault area agent cooperates with the down area agent and the line area agent to determine the power demand in the respective areas, employing the available power from the connecting lines. This complex process also depends on the switching mechanism and determines whether group repair or individual region repair is the most efficient course of action.

- **Lower area factor**

The agent situated in the lower region functions as an information conduit, which receives an information request message from the fault zone agent. Subsequently, it dispatches impedance and power demand data to the fault zone agent. Based on specific conditions, the lower region operator may receive signals instructing the opening or closing of switches in the regeneration zone. In a cohesive approach, the lower region agent sends out the information request message to the microgrid zone agents to obtain details regarding the zone demand or generation capacity of the microgrids, particularly in situations involving overload management.

- **Area line factor**

The zone line factor also plays a pivotal role in the recovery process. These agents employ their capabilities to gather information with the request call message from the fault zone agent. The information request message sent to the healthy zone agent during the recovery path requests the necessary data, including voltage, minimum voltage, impedance, and excess capacity. This information is very important in determining the allowable recovery power for each zone line operator.

- **Healthy area factor**

The agent in the healthy zone takes an active part in the healing process. The healthy zone agent computes the available surplus current and delivers data, comprising voltage, minimum voltage, impedance, and overload in the microgrids, upon receiving the information request message from the zone line agent. For the overload microgrid regional factor, the overload values, according to Eq. (27), are calculated to measure the amount of overload in the corresponding microgrid. On the other hand, the non-load microgrid regional factors calculate the production surplus in microgrids based on Eq. (28) [5]:

$$P_{Over}(n,\omega) = D_{MG}(n,t,\omega) - P_{MG}(n,t,\omega) \tag{27}$$

$$P_{Exe}(n,\omega) = P_{MG}(n,t,\omega) - D_{MG}(n,t,\omega) \tag{28}$$

Introducing energy trading between microgrids could provide additional flexibility and cost optimization. A new equation is proposed to model the energy trading mechanism between microgrids:

$$\begin{aligned}\mathrm{P_{Trade}}(\mathrm{m},\mathrm{n},\mathrm{t},\omega) = {} & \alpha_{\mathrm{mn}}(\mathrm{t},\omega) \\ & \times (\mathrm{P_{MG}}(\mathrm{m},\mathrm{t},\omega) \\ & - \mathrm{P_{Load}}(\mathrm{n},\mathrm{t},\omega))\end{aligned} \tag{29}$$

Where, $P_{Trade}(m,n,t,\omega)$ is the power traded from microgrid mmm to microgrid n at time t under scenario ω, $\alpha_{mn}(t,\omega)$ is the trading coefficient, which is a function of network capacity and market conditions, $P_{MG}(m,t,\omega)$ and $P_{Load}(n,t,\omega)$ are the power generation and load demands for microgrids m and n, respectively. This equation that the total energy traded does not exceed the available generation in each microgrid:

$$0 \leq \mathrm{P_{Trade}}(\mathrm{m},\mathrm{n},\mathrm{t},\omega) \leq \mathrm{P_{Trade}^{Max}} \tag{30}$$

The original cost minimization function can be modified to incorporate emissions reduction as a secondary objective. The new multi-objective function minimizes both operational cost and carbon emissions, using a weighted trade-off between the two objectives:

$$\min \sum_{\omega} \pi(\omega) \times \sum_{t} \left[\lambda(t,\omega) \times P_{Ref}^{S}(t,\omega) + \beta \sum_{m,n} P_{Trade}(m,n,t,\omega) \right] \tag{31}$$

Herein α and β signify the respective weight coefficients for cost and emissions. This modified objective function permits a balance between minimizing costs and decreasing emissions, which prepares a more comprehensive approach to sustainable energy management. The energy storage constraint can be expanded to account for degradation and charging/discharging efficiency, which changes over time:

$$E_{ES}(m,t+1,\omega) = \eta_{Ch} \times P_{Ch}^{ES}(m,t,\omega) + E_{ES}(m,t,\omega) - \frac{P_{Dch}^{ES}(m,t,\omega)}{\eta_{Dch}} \tag{32}$$

Herein $\eta_{Ch}(t,\omega)$ and $\eta_{Dch}(t,\omega)$ are time-varying efficiencies that decline as the storage system ages.

2.3. Uncertainty

In the first optimization stage, a different array of uncertainty parameters plays a significant role. These parameters comprise the active and reactive loads of the microgrids, the power generated by solar and wind turbines, the cost of energy, the rate and pressure at which EVs are charged, and the duration of time at which EVs are disconnected from the grid. A method of stochastic planning that is scenario-based is employed to justify the random character of these factors. Normal probability distribution functions are used to model the load parameters; beta and Weibull probability distribution functions are used to represent the production power of solar systems and wind; and Rayleigh distribution functions are used to describe the parameters of electric vehicles. The roulette wheel mechanism and the Kantorovich method, in addition to these distribution functions, aid in the generation and reduction of scenario samples and serve as a foundation for the optimization strategy:

$$P_{Load}(n,t,\omega) \sim \mathcal{N}\left(\mu_{P_{Load}}, \sigma_{P_{Load}}^2\right), \quad Q_{Load}(n,t,\omega) \sim \mathcal{N}\left(\mu_{Q_{Load}}, \sigma_{Q_{Load}}^2\right) \tag{33}$$

Where $P_{Load}(n,t,\omega)$ and $Q_{Load}(n,t,\omega)$ represent the active and reactive power load at node n, time t, and scenario ω, with respective mean μ and variance σ^2. The total power load for the distribution grid under uncertainty becomes:

$$P_{Total}(t,\omega) = \sum_{n} P_{Load}(n,t,\omega), \quad Q_{Total}(t,\omega) = \sum_{n} Q_{Load}(n,t,\omega) \tag{34}$$

The power generated by solar panels and wind turbines is highly variable. For solar power, a Beta distribution is used:

$$P_{PV}(t,\omega) \sim \mathrm{Beta}(\alpha_{PV}, \beta_{PV}) \tag{35}$$

For wind power, the generation is modeled utilizing the Weibull distribution:

$$P_{Wind}(t,\omega) \sim \mathrm{Weibull}(k_{Wind}, \lambda_{Wind}) \tag{36}$$

Thus, the total renewable power available at time tt under scenario ω is given by:

$$P_{RES}(t,\omega) = P_{PV}(t,\omega) + P_{Wind}(t,\omega) \tag{37}$$

The uncertainty in renewable generation requires scenario-based consideration for planning the grid's response.

The behavior of EVs, including the rate at which they charge or discharge and the time they remain connected to the grid, adds additional uncertainty. These factors are modeled using a Rayleigh distribution for the charging duration and rate:

$$T_{EV}(m,t,\omega) \sim \mathrm{Rayleigh}(\sigma_{T_{EV}}) \tag{38}$$

The power demand or supply from EVs during a given time interval t and scenario ω is:

$$P_{EV}(m,t,\omega) = P_{Ch}^{EV}(m,t,\omega) - P_{Dch}^{EV}(m,t,\omega) \tag{39}$$

Herein $P_{Ch}^{EV}(m,t,\omega)$ and $P_{Dch}^{EV}(m,t,\omega)$ represent the charging and discharging power of EVs.

To account for these uncertainties, a stochastic programming approach is used. The objective function to minimize the total operational cost COp, considering all possible scenarios ω, is given by:

$$\min \sum_{\omega} \pi(\omega) \cdot \sum_{t} C_{Op}(t,\omega) \tag{40}$$

In which π(ω) is the probability of scenario ω and COp(t,ω) is the operational cost at time t under scenario ω. The operational cost includes energy costs, renewable generation, and battery storage management, described as:

$$C_{Op}(t,\omega) = \lambda(t,\omega) \cdot (P_{Grid}(t,\omega) + P_{RES}(t,\omega)) + \sum_{n} (C_{EV}(t,\omega) + C_{ES}(t,\omega)) \tag{41}$$

The large number of potential scenarios due to these uncertainties is managed by scenario generation utilizing the roulette wheel mechanism. Scenario reduction is accomplished by employing the Kantorovich method, which minimizes the distance between the probability distributions of the full set of scenarios and the reduced set. This guarantees that the selected subset of scenarios accurately represents the overall uncertainty. The objective function for the reduced scenario set becomes:

$$\min \sum_{\omega' \in \Omega'} \pi(\omega') \cdot \sum_{t} C_{0p}(t, \omega') \tag{42}$$

Where Ω' is the reduced set of scenarios.

3. Optimization Algorithm

In the academic field, student performance is always evaluated by the grades they get in exams. The title of best student is awarded to the person who gets the highest grades and deserves it, as they are rewarded for their academic prowess. This recognition often acts as a strong motivator for the other students in the class, instilling in them the desire to improve their performance and compete for the prestigious title of best student. The path to becoming the best student is not without challenges. To achieve this title, students must invest significant effort in each subject that makes up their academic curriculum. This serious effort spans the entire duration of their training. It is a period marked by dedication, focus, and consistent hard work all focused to improve their performance in a spectrum of subjects at their disposal. Formulation of the concept on the optimization algorithm based on the student's psychology can be set based on the perception of student psychology and excellence. Under the attainment of the title of the best student, there is an important consideration of doing more desirable compared to others. In achieving this, it will require students to adjust the effort in each subject. Their commitment can range depending on personal capabilities, predispositions, and enthusiasm concerning a certain subject. One owes it to this fact that the means or the way to higher achievement at examinations is not similar but rather it is a path which is built through some sort of Psychology and approach that a student has. Students' strategies for improvement are influenced by their individual psychological tendencies. Some students strive to match or surpass the best student's efforts in a subject, believing that imitation is their ticket to success. Others, in contrast, set their sights higher, go beyond the best student's efforts, and direct their energy toward outperforming their peers, who make up the average class performance. Allocating effort to subjects becomes a strategic game that is closely tied to students' interests and ambitions. Therefore, the overall increase in student performance is intrinsically related to the effort expended in each subject. As a result, students in any given class can be classified into four distinct groups, as shown in Fig. 1.

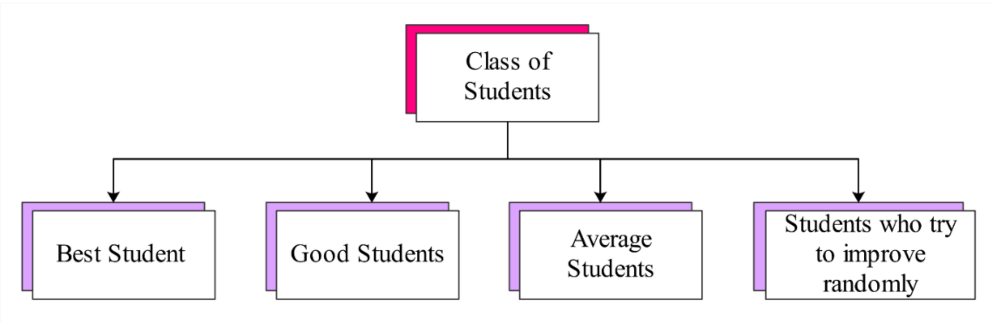

Fig. 1. Classification of students in a class.

I. **Top student:** The top student consistently pursues the highest grades. To maintain this position, the best student must put more effort into each subject than his peers. The performance increase of the best student can be specified by Eq. (43), which includes the dynamic relationship between the best student and randomly selected students. In this relation, X^{Best} is the performance of the best student, X(j) is the performance of random student j, *Rand* is a random number between 0 and 1, and k is a parameter that is considered randomly as either 1 or 2 [27]:

$$X_{New}^{Best} = X^{Best} + Rand \times (-1)^k \times (X^{Best} - X(j)) \tag{43}$$

II. **Good Student:** Students who show a particular passion for a subject direct their efforts towards excellence in that area, thus increasing their overall performance. The category of good students is a dynamic category that reflects the psychology of different students. The goal of some good students is to match or surpass the best student's efforts, as shown by Eq. (44). Others aim higher by trying harder than the average student in the class the relevant relationship is shown in Eq.

(45), where X^{Mean} represents the average performance of the class [27]:

$$X_{New}(i) = X^{Best} + Rand \times (X^{Best} - X(i)) \quad (44)$$

$$X_{New}(i) = X(i) + Rand \times (X^{Best} - X(i)) + Rand \times (X(i) - X^{Mean}) \quad (45)$$

III. **Average student:** Students in this category allocate their efforts based on their interests and spend average energy on subjects that do not interest them. These students compensate by allocating extra effort to other subjects to improve overall performance. The manifestation of middle school students is intrinsically related to students' psychological tendencies. Their performance characteristics can be determined by Eq. (46) [27]:

$$X_{New}(i) = X(i) + Rand \times (X^{Mean} - X(i)) \quad (46)$$

IV. Random Progress Seekers: Along with these three categories of student patterns, a unique group of students takes a more unorthodox approach. They pursue improved performance through random attempts across subjects, allowing for a varied and flexible approach. Their performance is represented by Eq. (47), where X^{Min} and X^{Max} consider the minimum and maximum limits of a subject.

$$X_{New}(i) = X^{Min} + Rand \times (X^{Max} - X^{Min}) \quad (47)$$

To improve the optimization process, a Local Search Strategy can be incorporated to fine-tune the performance of each student (solution). This local search is designed to explore the neighborhood of a given solution by adjusting the performance slightly based on nearby students' performances. This step ensures that the solutions are not just globally driven but also locally optimized. The local search mechanism is applied to each student by considering the performances of its neighboring students. The adjustment is guided by a small perturbation factor and the average performance of nearby students:

$$X_{NewLocal}(i) = X(i) + \alpha \times \left(\frac{1}{N}\sum_{j=1}^{N} X(j) - X(i)\right) + \beta \times Rand \quad (48)$$

Where X(i) symbolizes the current performance of student i. N is the number of neighboring students considered for local search. α is a local search control parameter (a small positive number to control the magnitude of adjustments). $\sum_{j=1}^{N} X(j)$ is the sum of the performances of the neighboring students. β is a random perturbation factor. Rand is a random number between 0 and 1. The first term of the above equation reflects the difference between the average performance of neighboring students and the current student ii's performance. This helps in pulling the current solution towards the local optimum. The second term β×Rand introduces a random perturbation to escape potential local optima. In the global search, each student's performance is adjusted by considering both the best-performing student and the worst-performing student in the class. This strategy enables exploration of solutions far from the current point, increasing the chances of finding a better solution:

$X_{NewGlobal}(i) = X(i) + \gamma \times (X^{Best} - X^{Worst}) + \delta \times Rand$	(49)

Herein X(i) is the current performance of student i. X^{Best} signifies the performance of the best student in the class. X^{Worst} is the performance of the worst student in the class. γ is the global search control parameter (positive number, generally larger than the local search parameter, to encourage bigger jumps). δ is a random perturbation factor to allow exploration in a random direction. Rand is a random number between 0 and 1.

4. Numerical analysis

As can be seen in Fig. 2, the suggested recovery approach has been applied in the IEEE 33-bus radial distribution network [28], where the voltage is 12.66 kV and the base power is 1 MW, within the framework of this study. After being regarded, 0.9 pu and 1.05 pu have been established as the minimum and maximum voltage limitations for each bus, respectively. Every bus is deliberately positioned between two switches, as illustrated in Fig. 2, so every bus is a zone agent. To evaluate the electrical characteristics of the network and compliance with the operating limits, load distribution calculations were performed using the backward method implemented in the MATLAB software environment. The network's line voltage and current restrictions were validated by this investigation. It has been assumed that there are four microgrids in this network, which are housed in buses 23, 25, 28, and 30. Each microgrid's load is equal to the bus's load that corresponds to it at that point. In addition, EVs were included in the network with 21 units on bus 23, 60 units on bus 25, 21 units on bus 28, and 30 units on bus 30. In addition, two strategies have been introduced for EV charging management based on references [29,30]:

- **Strategy A:** EVs start the charging process after connecting to the grid and disconnect after their batteries are fully charged.
- **Strategy B:** EVs are varied according to the energy prices and network functional constraints. This strategy is designed to optimize charging costs and promote the integration of EVs into the grid.

The daily contribution of the EV penetration rate for the suggested techniques is displayed in Fig. 3. This graph shows how quickly EVs are being integrated into the grid [30].

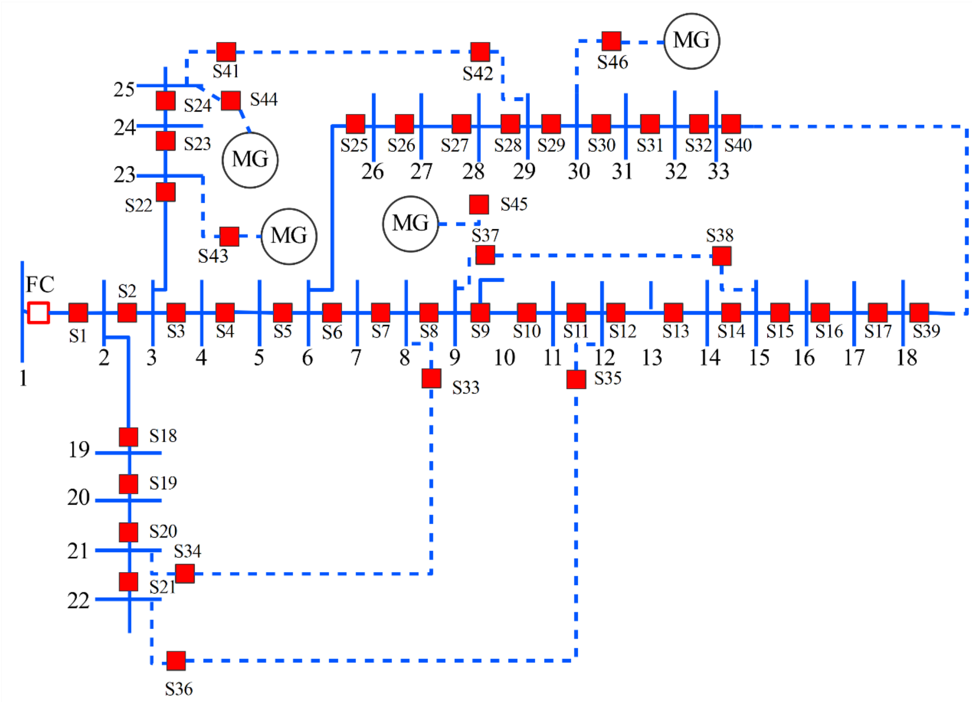

Fig. 2. The system of 33 tires under study.

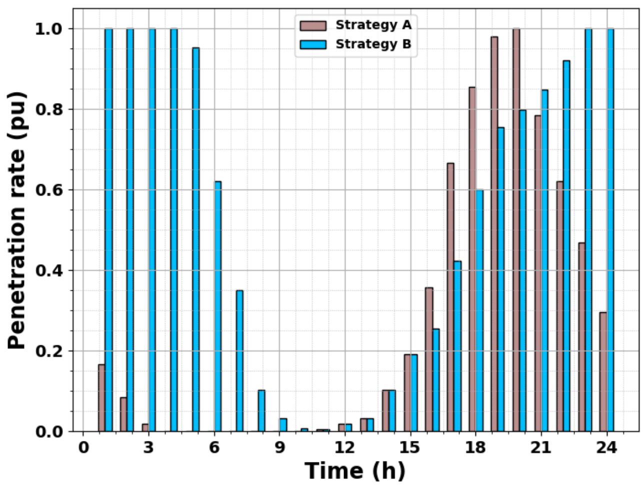

Fig. 3. Participation rate of Evs.

Fig. 4 [31] displays the load, photovoltaic, and wind turbine power distribution. Furthermore, the details of the estimated daily energy price are provided in [32]. It is assumed for this analysis that these microgrids have 400 kWh, 900 kWh, 400 kWh, and 500 kWh of batteries, each of which runs at an efficiency of 0.89. The solar resources have capacities of 270 kW, 710 kW, 250 kW, and 340 kW, and the wind resources have capacities of 330 kW, 800 kW, 330 kW, and 510 kW. The voltage limits of 0.9 pu to 1.05 pu are established based on standard practices such as those outlined in IEEE Standard 1547. These limits are designed to guarantee that voltage remains inside a range that supports system reliability and equipment safety.

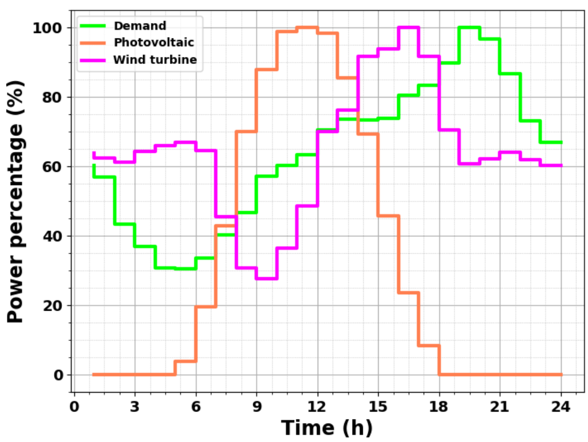

Fig. 4. Renewable production and hourly network load.

4.1. Optimal coordination of integrated neighborhood microgrids using the proposed comprehensive energy management algorithm

This section provides valuable insights into the results of our analysis, especially regarding the optimal coordination of integrated neighborhood microgrids employing the proposed comprehensive EM algorithm. Figs 5 and 6 suggest a detailed visual representation of the predicted overload power and stored energy in the microgrids under two diverse strategies: Strategy A and Strategy B. Fig. 5 outlines the performance under Strategy A. Panel (a) shows the overload power experienced by the microgrid at bus 25, which indicates that significant overload occurs at 20:00 and 21:00. This overload is linked to peak load conditions, primarily because of the increased EV charging between 17:00 and 22:00, as highlighted in Fig.3. Panel (b) of Fig. 5 depicts the stored energy in the microgrids located at buses 23, 28, and 30 during the same period. The energy storage levels consistently exceed 50 kWh from 20:00 to 24:00. This surplus energy is essential to alleviate the overload in the microgrid at bus 25, which demonstrates how the additional stored energy can be utilized to manage the peak load. Fig. 6 brings out the outputs under Strategy B. Panel (a) depicts the overload power for the microgrid at bus 25, which shifts to occurring at 03:00. This shift is associated with a significant increase in EV charging during off-peak hours (01:00 – 07:00), a period characterized by favorable energy prices. Panel (b) of Fig. 6 shows that, despite the overload power reaching approximately 6.8 kWh, the stored energy in the microgrids at buses 23, 28, and 30 remains well above 200 kWh. This ample stored energy is more than sufficient to address the overload conditions in the microgrid at bus 25, which demonstrates the effectiveness of Strategy B in utilizing stored energy to manage overload situations. Table 1 complements these figures by providing a summary of the results related to overload management. It details the expected unsupplied energy for the microgrid at bus 25, with Strategy A which shows an expected unsupplied energy of 108.48 kWh, while Strategy B significantly decreases this to 7.21 kWh. Moreover, Table 1 lists the total minimum energy stored in other microgrids, which is calculated at 172.03 kWh for Strategy A and 220.94 kWh for Strategy B. These are considerably higher than the expected unsupplied energy at the two strategies and makes the energy stored in microgrids at buses 23, 28, and 30 quite adequate to meet the expected load demand at bus 25. In totality, this study demonstrates that a proposed complete-site EM algorithm operates overload conditions in interconnected neighborhood microgrids to bring a reduction in an expected unsupplied energy with overall minimum energy costs.

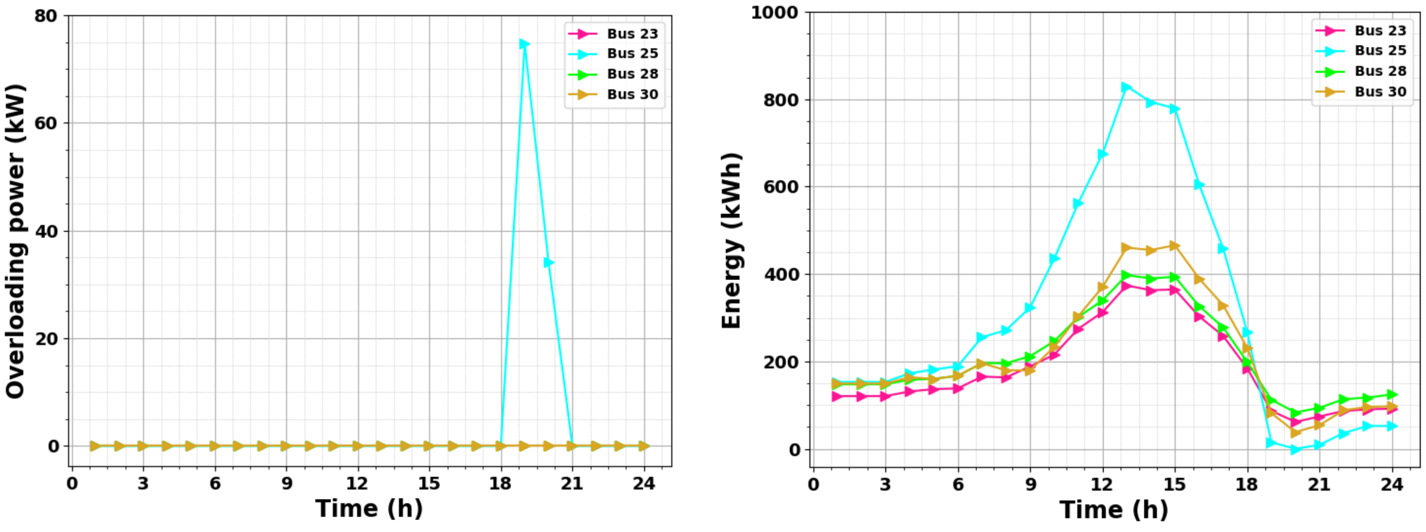

(a) Overloading power (b) Energy stored in battery

Fig. 5. Results obtained for each microgrid using strategy A.

.

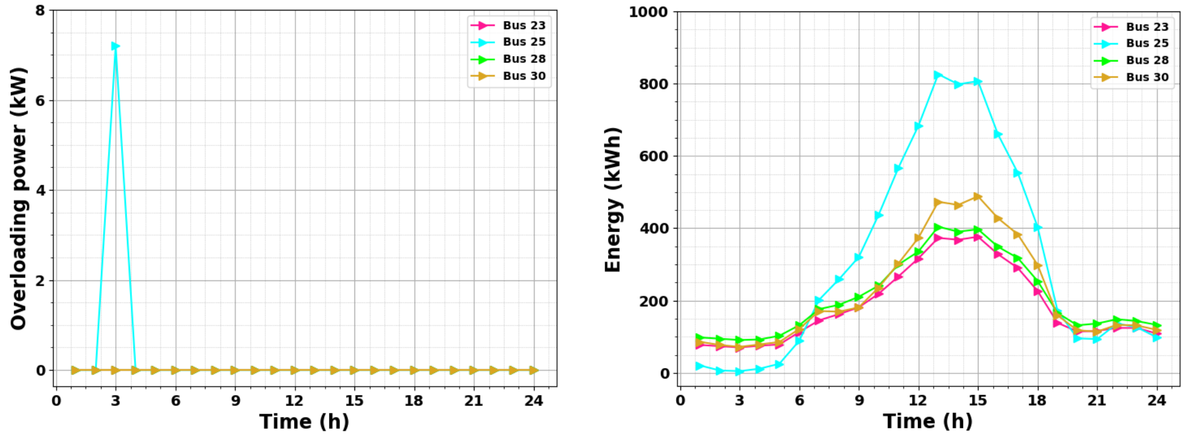

(a) Overloading power (b Energy stored in battery

Fig. 6. Obtained results for each microgrid using strategy B.

Table 1. Obtained results using different strategies and approaches.

Strategy		A	B
Non-overloading	Bus	23, 28, 30	23, 28, 30
	Minimum stored energy (kWh)	54.2, 80.1, 38.1	67.1, 88.12, 66.93
	Total stored energy in microgrids (kWh)	172.03	220.94
Overloading before coupling neighboring microgrids management	Bus	25	25
	Expected energy not supplied (kWh)	108.48	7.21
Overloading after coupling neighboring microgrids management	Bus	25	25
	Expected energy not supplied (kWh)	0	0

4.2. Using the synergy of comprehensive energy management algorithm and SHS

This section evaluates the proposed multi-agent system with autonomous distributed regeneration technology capability in a two-stage configuration that integrates a comprehensive EM algorithm and SHS. To express results in this part, two separate case studies are considered:

- Case study 1: This case study separately investigates the capacity of the proposed multi-agent system with the capability of autonomous distributed restoration technology.
- Case Study 2: This case study investigates the potential of the proposed multi-agent system with autonomous distributed restoration technology capability when coordinated with a comprehensive EM algorithm and SHS.

In case study 1, the evaluation focuses on the performance and efficiency of the proposed recovery method. Specifically, this method is applied to a 33-bus network without considering neighboring microgrids. When a fault occurs in this network, the circuit breaker of the faulted part is the first equipment to turn off. After that, the fault location switches are opened to isolate the affected area from the network. Following these changes, the fault location switches communicate with the fault segment circuit breaker, which recloses the upstream zones of fault location switches. It then initiates the recovery process and the switches at the fault location send a message to the downstream zone agent to calculate the load. The results of this initial stage are presented in Table 2. It is important to note that if a fault occurs in the last feeder area, such as bus 33 in a 33-bus network, the rebuild process is unnecessary. In such cases, the downstream area load is zero. However, for other fault locations, such as bus 20, 16, and 11, the total load of the downstream area is calculated, which represents the load to be recovered.

Table 2. Information of the switches of fault location and agent of downstream area.

Faulted bus	Down zone agent	Total apparent power of downward zone agent	Available restoration tie
11	12 - 18	56.73 KVA	(9, 15), (12, 22) and (18, 33)
16	17 and 18	16.12 KVA	(33, 28)
20	21 and 22	19.65 KVA	(8, 21) and (12, 22)
33	-	0	-

In case study 2, the performance of the proposed method was examined in the worst-case scenario. This scenario assumes that the fault occurs on bus 24 at 20:00 for EV charging strategy A and at 03:00 for strategy B in neighborhood microgrids. The integration of the comprehensive EM algorithm and the SHS makes the fault component turn off and region 24 is determined as the fault region factor. Switches s23 and s24 are opened for isolating zone 24 from the network. The fault component is then informed to reclose the regions upstream of the fault region including regions 2, 3, and 23. The rebuild process is initiated by sending a rebuild start message to the agent of the lower zone or the zone located on bus 25. which according to Table 1 has overload conditions at specified times. The lower zone agent requests the overload microgrid zone agent to obtain the microgrid load demand on bus 25. The overloaded microgrid zone agent, in turn, sends a regeneration initiation message to the non-overloaded microgrid zone agents located on buses 23, 28, and 30 to provide the overload power required by the microgrid on bus 25. The results of these examinations show that the proposed recovery method effectively manages the constraints of network operation. The maximum voltage deviation for both strategies A and B is less than the limit of 0.1 pu. In addition, the values of the minimum allowable current remain positive, which indicates that the proposed method successfully adheres to the grid line current limit.

4.3. Sensitivity Analysis

In this study, a comprehensive sensitivity analysis was conducted to evaluate how variations in key parameters, including RES penetration and ESS capacities, affect the performance of the system.

The research investigated the impacts of different levels of RES penetration on system performance. The RES capacities (solar and wind) were adjusted to 50%, 75%, 100%, and 125% of the baseline values to perceive their impact on system reliability and overload conditions. At 50% RES penetration, the expected unsupplied energy raised to 152.37 kWh, and peak overloads at bus 25 rose to 8.4 kWh during peak hours (21:00). The minimum stored energy in the microgrids dropped to 140.52 kWh, which reflects a decreased capacity to manage peak loads. As RES penetration increased to 75%, the expected unsupplied energy declined to 110.54 kWh, and peak overloads at bus 25 reduced to 6.9 kWh. The minimum stored energy increased to 170.31 kWh, which shows an improved ability to overcome load oscillations. At 100% RES penetration, the expected unsupplied energy was 108.48 kWh, with peak overloads at bus 25 at 6.8 kWh and minimum stored energy at 172.03 kWh. Increasing RES penetration to 125% further reduced the expected unsupplied energy to 87.22 kWh and peak overloads to 5.5 kWh, while the minimum stored energy rose to 203.45 kWh. These outputs highlight that higher RES penetration improves the system's capability to manage overload conditions and improves energy availability, which is crucial for maintaining system reliability.

The impact of varying ESS capacities was also assessed. ESS capacities were adjusted to 50%, 75%, 100%, and 125% of the baseline values to determine their effect on overload management and energy supply reliability. When ESS capacities were reduced to 50% of the baseline, the expected unsupplied energy increased to 132.15 kWh, and peak overloads at bus 25 reached 7.9 kWh. The minimum stored energy fell to 122.81 kWh, indicating a diminished capacity to buffer against overloads. At 75% ESS capacity, the expected unsupplied energy decreased to 115.09 kWh, and peak overloads were reduced to 6.7 kWh, with minimum stored energy increasing to 150.67 kWh. With ESS capacities at 100% of the baseline, the expected unsupplied energy was 108.48 kWh, peak overloads at bus 25 were 6.8 kWh, and minimum stored energy was 172.03 kWh. Growing ESS capacities to 125% further reduced the expected unsupplied energy to 94.11 kWh and peak overloads to 5.2 kWh, while minimum stored energy rose to 201.89 kWh. This examination underscores that larger ESS capacities improve the system's ability to manage overloads and reduce unsupplied energy, which depicts the significance of sufficient energy storage in maintaining system performance.

Overall, the sensitivity analysis outlines that higher RES penetration and increased ESS capacities significantly elevate system performance. These adjustments lead to more favorable management of overload conditions and decreased expected unsupplied energy, thereby improving the reliability and efficiency of the smart distribution network.

5. Conclusion

This paper introduced a novel method that combined the SHS in the SDN with the two-step implementation of the comprehensive energy management algorithm. This network utilized a multi-agent system with a self-governing distributed regeneration method and was made up of local microgrids. Regarding comprehensive energy management, each microgrid consisted of various components, including load components, renewable energy systems, energy management charging framework, and energy storage systems. The decrements in network operation costs were the primary objective of this examination's first phase. To accomplish the mentioned objective, the problem was put through predetermined system utilization restrictions, optimal network load distribution equations, and neighborhood microgrid-specific constraints. The purpose of the presented evaluation was to optimize the SDN's efficient function pondering these viewpoints, especially when it comes to neighborhood microgrids. In the second step, the focus shifted to the optimization of regeneration processes using the multi-agent system combined with the proposed autonomous distributed regeneration technology. Reducing the discrepancy between recoverable priority loads and the number of switching operations was the primary goal. The optimization process took into account limitations related to system use, recovery requirements, and network limits. Furthermore, this work presented a strong approach to modeling and managing uncertainty in many problem domains through stochastic programming approaches, which generated and reduced scenarios with the assistance of the Kantorovich method and the roulette wheel mechanism. By considering uncertainties, this study increased the reliability of the proposed reliability method. It should be noted that the formulation of both the first and second stages of this study is non-linear. To find a solution that meets the requirements of the problem while keeping the solution deviation low, this study utilized an optimization algorithm based on student psychology. This algorithm helped to arrive at a safe and reliable solution to the complex problem at hand. The study's numerical findings demonstrated how well the suggested recovery strategy works in the distribution network to keep line current and voltage through allowable bounds, especially in the case of a fault. It not only facilitated a smart distribution grid but also effectively managed the overload challenges associated with neighborhood microgrids, which ultimately assisted in forming a more reliable and resilient grid.

Reference

1. Mohammad Zaheri D, Nazerian Salmani S, Shahnia F, Wang H, Su X. A Two-Stage Hybrid Stochastic–Robust Coordination of Combined Energy Management and Self-Healing in Smart Distribution Networks Incorporating Multiple Microgrids. Energies (Basel) 2024;17:4281. https://doi.org/10.3390/en17174281.
2. Nourian S, Kazemi A. A two-stage optimization technique for automated distribution systems self-healing: Leveraging internet data centers, power-to-hydrogen units, and energy storage systems. J Energy Storage 2024;85:111084. https://doi.org/10.1016/j.est.2024.111084.
3. Ghasemi-Marzbali A, Ahmadiahangar R, Orimi SG, Shafiei M, Häring T, Rosin A. Energy Management of an Isolated Microgrid: A Practical Case. IECON 2021 – 47th Annual Conference of the IEEE Industrial Electronics Society, 2021, p. 1–6. https://doi.org/10.1109/IECON48115.2021.9589801.
4. Lu J, Zhao R, Guo W, Li H, Hu B, Lin J. Uniform design-based self-healing evaluation for active distribution network. Electric Power Systems Research 2024;235:110863.
5. Mohammad Zaheri D, Khederzadeh M. Two-stage coupling of coordinated energy management and self-healing strategies in a smart distribution network considering coupling neighbouring microgrids according to autonomous decentralized restoration technique. International Transactions on Electrical Energy Systems 2020;30:e12596.
6. Zhao R, Tan Y, Lu J, Guo W, Du H. A resilient self-healing approach for active distribution networks considering dynamic microgrid formation. Energy Sci Eng 2024;12:230–48. https://doi.org/10.1002/ese3.1631
7. Wong J, Tan C, Rahim NA, Tan RHG. A Communication-less adaptive protection scheme for Self-Healing distribution systems. International Journal of Electrical Power & Energy Systems 2023;148:108992.
8. Yavuz L, Soran A, Önen A, Li X, Muyeen SM. Adaptive fault detection scheme using an optimized self-healing ensemble machine learning algorithm. CSEE Journal of Power and Energy Systems 2021;8:1145–56.
9. Srivastava I, Bhat S, Vardhan BVS, Bokde ND. Fault detection, isolation and service restoration in modern power distribution systems: A

review. Energies (Basel) 2022;15:7264. https://doi.org/10.3390/en15197264

10. Arefifar SA, Alam MS, Hamadi A. A review on self-healing in modern power distribution systems. Journal of Modern Power Systems and Clean Energy 2023;11:1719–33. https://doi.org/10.35833/MPCE.2022.000032
11. Esmail EM, Elkalashy NI, Kawady TA, Taalab A-MI, Elsadd MA. Modified autonomous fault management strategy for enhancing distribution network reliability. Electrical Engineering 2022:1–16. https://doi.org/10.1007/s00202-021-01216-6
12. Wong J, Tan C, Rahim NA, Tan RHG. A Communication-less adaptive protection scheme for Self-Healing distribution systems. International Journal of Electrical Power & Energy Systems 2023;148:108992.
13. Aldrini J, Chihi I, Sidhom L. Fault diagnosis and self-healing for smart manufacturing: a review. J Intell Manuf 2024;35:2441–73. https://doi.org/10.1007/s10845-023-02165-6
14. Mahmoud MA, Md Nasir NR, Gurunathan M, Raj P, Mostafa SA. The current state of the art in research on predictive maintenance in smart grid distribution network: Fault's types, causes, and prediction methods—A systematic review. Energies (Basel) 2021;14:5078. https://doi.org/10.3390/en14165078
15. Kuo M-T. Application of the artificial bee colony algorithm to scheduling strategies for energy-storage systems of a microgrid with self-healing functions. IEEE Trans Ind Appl 2021;57:2156–67. https://doi.org/10.1109/TIA.2021.3058233
16. Zakaryaseraji M, Ghasemi-Marzbali A. Evaluating congestion management of power system considering the demand response program and distributed generation. International Transactions on Electrical Energy Systems 2022;2022:5818757.
17. Shittu E, Tibrewala A, Kalla S, Wang X. Meta-analysis of the strategies for self-healing and resilience in power systems. Advances in Applied Energy 2021;4:100036.
18. Nahi S, Zare K, Faghihi F. Self-healing service for lowest load shedding in distribution networks using responsive loads and subcontractor feeder. Sustainable Energy, Grids and Networks 2022;32:100863.
19. Sardashti A, Ramezani A. Fault tolerant control of islanded AC microgrids under sensor and communication link faults using online recursive reduced-order estimation. International Journal of Electrical Power & Energy Systems 2021;126:106578.
20. El-Tawab S, Saad H, Abdel-Aziz AM. Network Self-Healing by Fault Detection and Clearing using Different Topologies to restore the System n.d. https://doi.org/10.13140/RG.2.2.32448.55041.
21. [21] Shyama M, Pillai AS, Anpalagan A. Self-healing and optimal fault tolerant routing in wireless sensor networks using genetical swarm optimization. Computer Networks 2022;217:109359.
22. Aldrini J, Chihi I, Sidhom L. Fault diagnosis and self-healing for smart manufacturing: a review. J Intell Manuf 2024;35:2441–73. https://doi.org/10.1007/s10845-023-02165-6
23. Guan L, Chen H, Lin L. A multi-agent-based self-healing framework considering fault tolerance and automatic restoration for distribution networks. IEEE Access 2021;9:21522–31. https://doi.org/10.1109/ACCESS.2021.3055284
24. Fan D, Ren Y, Feng Q, Liu Y, Wang Z, Lin J. Restoration of smart grids: Current status, challenges, and opportunities. Renewable and Sustainable Energy Reviews 2021;143:110909.
25. Thirunavukkarasu M, Sawle Y, Lala H. A comprehensive review on optimization of hybrid renewable energy systems using various optimization techniques. Renewable and Sustainable Energy Reviews 2023;176:113192.
26. Hasankhani A, Hakimi SM, Bisheh-Niasar M, Shafie-khah M, Asadolahi H. Blockchain technology in the future smart grids: A comprehensive review and frameworks. International Journal of Electrical Power & Energy Systems 2021;129:106811.
27. Das B, Mukherjee V, Das D. Student psychology based optimization algorithm: A new population based optimization algorithm for solving optimization problems. Advances in Engineering Software 2020;146:102804.
28. Babu PR, Rakesh CP, Kumar MN, Srikanth G, Reddy DP. A novel approach for solving distribution networks. 2009 Annual IEEE India Conference, IEEE; 2009, p. 1–5. https://doi.org/10.1109/INDCON.2009.5409363
29. Pirouzi S, Aghaei J. Mathematical modeling of electric vehicles contributions in voltage security of smart distribution networks. Simulation 2019;95:429–39. https://doi.org/10.1177/0037549718778766
30. Pirouzi S, Aghaei J, Niknam T, Farahmand H, Korpås M. Exploring prospective benefits of electric vehicles for optimal energy conditioning in distribution networks. Energy 2018;157:679–89. https://doi.org/10.1016/j.energy.2018.05.195
31. Yan Q, Qian C, Zhang B, Kezunovic M. Statistical analysis and modeling of plug-in electric vehicle charging demand in distribution

systems. 2017 19th International Conference on Intelligent System Application to Power Systems (ISAP), IEEE; 2017, p. 1–6. https://doi.org/10.1109/ISAP.2017.8071365

32. Pirouzi S, Aghaei J, Vahidinasab V, Niknam T, Khodaei A. Robust linear architecture for active/reactive power scheduling of EV integrated smart distribution networks. Electric Power Systems Research 2018;155:8–20. https://doi.org/10.1016/j.epsr.2017.09.021

Acronyms	
Abbreviations	
ATC	Available Transfer Capability
DG	Distributed Generation
EM	Energy Management
ESS	Energy Storage Systems
EV	Electric Vehicles
RES	Renewable Energy Systems
SDN	Smart Distribution Network
SHS	Self-Healing System
Symbols	
π	Probability of scenario
λ	Energy price
B	Incidence matrix of bus microgrid
A	Incidence matrix of bus-line based on the current direction
g	Conductance of a line
P_D	Active load
Q_D	Reactive load
V_{Ref}	Voltage of slack bus
I_{VH}	The maximum current of a healthy feeder neglecting the violation of the voltage limit
I_{VF}	The maximum current of the fault feeder neglecting the violation of the voltage limit
S_L^{Max}	Maximum capacity of distribution line
S_S^{Max}	Maximum capacity of distribution station
V^{Min}	Minimum voltage magnitude
V^{Max}	Maximum voltage magnitude
η_{Ch}	Charging efficiency
η_{Dch}	Discharging efficiency
CR^{EV}	Charge rate of electric vehicles
DR^{EV}	Discharge rate of electric vehicles
E^{Max}	Maximum energy of the battery
E^{Min}	Minimum energy of the battery
CR^{ES}	Charge rate of battery
DR^{ES}	Discharge rate of battery
Variables	
P_S	Active power of distribution station
P_{MG}	Active power of microgrid
P_L	Active power flow of distribution line
Q_S	Reactive power of distribution station
Q_L	Reactive power flow of distribution line
V	Voltage magnitude
δ	Voltage angles
P_{Ch}^{EV}	Charging active power of electric vehicles
P_{Dch}^{EV}	Discharging active power of electric vehicles
E^{Arr}	Initial energy of electric vehicles
E^{Dep}	Final energy of electric vehicles
P_{Ch}^{ES}	Charging active power of battery
P_{Dch}^{ES}	Discharging the active power of the battery
P_{PV}	Active power of the solar system
P_W	Active power of wind system
sw	Binary parameter of switch status